UC Berkeley
UC Berkeley Previously Published Works

Title

Impact of Error in Lidar-Derived Canopy Height and Canopy Base Height on Modeled Wildfire Behavior in the Sierra Nevada, California, USA

Permalink

Journal

ISSN

Authors

Kelly, Maggi
Su, Yanjun
Di Tommaso, Stefania
et al.

Publication Date

2018

DOI

Peer reviewed

remote sensing

MDPI

Impact of Error in Lidar-Derived Canopy Height and Canopy Base Height on Modeled Wildfire Behavior in the Sierra Nevada, California, USA

Maggi Kelly [1,2,*] (ID), **Yanjun Su [3,4], Stefania Di Tommaso [1], Danny L. Fry [1], Brandon M. Collins [5], Scott L. Stephens [1] and Qinghua Guo [3,4]**

[1] Department of Environmental Science, Policy, and Management, University of California, Berkeley, CA 94720-3114, USA; stefaniaditom@gmail.com (S.D.T.); dfry@berkeley.edu (D.L.F.); sstephens@berkeley.edu (S.L.S.)

[2] Division of Agriculture and Natural Resources (UCANR), University of California, Berkeley, CA 94720-3114, USA

[3] State Key Laboratory of Vegetation and Environmental Change, Institute of Botany, Chinese Academy of Sciences, Beijing 100093, China; suyanjun1987@gmail.com (Y.S.); guo.qinghua@gmail.com (Q.G.)

[4] Sierra Nevada Research Institute, School of Engineering, University of California at Merced, Merced, CA 95343, USA

[5] Center for Fire Research and Outreach, University of California, Berkeley, CA 94720-3114, USA; bcollins@berkeley.edu

[*] Correspondence: maggi@berkeley.edu; Tel.: +1-510-642-7272

Abstract: Light detection and ranging (Lidar) data can be used to create wall-to-wall forest structure and fuel products that are required for wildfire behavior simulation models. We know that Lidar-derived forest parameters have a non-negligible error associated with them, yet we do not know how this error influences the results of fire behavior modeling that use these layers as inputs. Here, we evaluated the influence of error associated with two Lidar data products—canopy height (CH) and canopy base height (CBH)—on simulated fire behavior in a case study in the Sierra Nevada, California, USA. We used a Monte Carlo simulation approach with expected randomized error added to each model input. Model 1 used the original, unmodified data, Model 2 incorporated error in the CH layer, and Model 3 incorporated error in the CBH layer. This sensitivity analysis showed that error in CH and CBH did not greatly influence the modeled conditional burn probability, fire size, or fire size distribution. We found that the expected error associated with CH and CBH did not greatly influence modeled results: conditional burn probability, fire size, and fire size distributions were very similar between Model 1 (original data), Model 2 (error added to CH), and Model 3 (error added to CBH). However, the impact of introduced error was more pronounced with CBH than with CH, and at lower canopy heights, the addition of error increased modeled canopy burn probability. Our work suggests that the use of Lidar data, even with its inherent error, can contribute to reliable and robust estimates of modeled forest fire behavior, and forest managers should be confident in using Lidar data products in their fire behavior modeling workflow.

Keywords: wildfire burn probability; crown fire; forest fuels; Sierra Nevada; Lidar; error

1. Introduction

Fire is an important component of forest ecosystems in western North America. Fire impacts on these ecosystems are predicted to increase as forests respond to a legacy of past management practices and increased drought stress that is associated with a changing climate [1–5]. Spatially explicit fire

behavior and effects modeling software packages (hereafter called "fire behavior models") are the primary planning tools used by forest fire managers to simulate fire spread across landscapes and to anticipate the effects of fuel reduction treatments to possibly slow down fire spread and reduce the fire intensity in a forest [6–11]. These tools are also increasingly used in other forest science domains, such as assessing fire impacts on wildlife habitat and on carbon dynamics [12,13]. In the United States (US), fire managers use wildfire behavior models to aid in fire management decision-making, to plan, allocate, and mobilize suppression resources, and to plan fuel reduction treatments across landscapes [14–16]. Fire behavior models include BEHAVE [17], FARSITE [18], and FlamMap [19].

1.1. Spatial Inputs to Fire Behavior Models

In addition to spatial data depicting topography (i.e., elevation, slope, and aspect), fire behavior models require spatial layers depicting forest structure and fuel characteristics [14,20]. These inputs data include canopy cover, canopy height, canopy base height, canopy bulk density, and fuels [21]. Canopy height (the average height of overstory trees) influences wind profiles within the forest; canopy base height (the height above which there is sufficient fuel to allow for vertical fire movement through the canopy) is critical in determining whether fire can reach the crowns of trees; and, canopy bulk density (the density of the canopy fuels that would be consumed in the flaming front of a fully active crown fire) quantifies the fuel in the canopy layer, which will feed active crown fires [22]. These metrics of forest structure are typically generated by entering data from field plots into forest growth models, such as the Fire and Fuels Extension in Forest Vegetation Simulator (FVS) [23], which use allometry to calculate the specific metrics. Often the metrics derived from field plots are assumed to represent a given vegetation patch, referred to as a stand. However, stand-level forest structure variables are not easily estimated or measured in the field [24]. For example, canopy bulk density cannot be measured directly [21], and is estimated based on tree crown dimensions, foliage and fine branch biomass. Calculations of canopy base height and canopy bulk density are based on certain assumptions, such as the shapes of tree crowns, the inclusion or not of seedlings, the vertical distribution of foliage and fine branches within tree crowns, and the threshold biomass density used to define the base of the canopy. These assumptions can lead to errors in the calculation of these variables, and in their spatial representation over a given stand [22,25]. However, such errors are not typically considered when interpolated data are used in fire behavior models [7,8,12,13,26].

1.2. Lidar to Measure Forest Structure

The use of Light Detection and Ranging (Lidar) for forest structure mapping provides an alternative protocol for data layer creation for fire behavior models than what is typically used. Instead of an interpolated product, Lidar data provides a spatially complete and precise measurement or model (via regression) of many aspects of forest structure and fuels over landscape scales that can be evaluated for measured accuracy when compared to data from field plot networks [20,27–29]. While it is possible to use model-based methods to upscale forest parameters from Lidar footprints to areas without Lidar coverage, for example [30–33], regression-based methods are still the most commonly unbiased method for extracting forest parameters in areas with extensive field plots. For example, researchers used Lidar to predict canopy base height (R^2 = 0.77; RMSE = 4.1 m) and canopy height (R^2 = 0.98; RMSE = 1.5 m), among other variables, in a western hemlock forest in Washington State [27]. Others analyzed Lidar data from Sierra Nevada forests to extract canopy stand height with moderate success (R^2 = 0.75, RMSE = 6.4 m) [34]. In Washington State, researchers examined canopy fuel metrics in a mixed-conifer forest and reported good prediction rates for canopy height (R^2 = 0.94; RMSE = 1.86 m) and canopy base height (R^2 = 0.78; RMSE = 0.68 m) [35]. This study was done in an even aged plantation and reported better results for physical measurements (e.g., max height, basal area, and canopy cover) than for modeled estimates (e.g., canopy base height). Using the same Lidar data as presented here, researchers provided a review of the prediction ability of Lidar metrics for a suite of forest structural variables. The best prediction rates were associated with maximum canopy

height (R^2 = 0.87), basal area (R^2 = 0.82), and canopy cover (R^2 = 0.85) [20]. Canopy base height prediction was more problematic with R^2 = 0.41. From these and other projects we understand that retrieving accurate forest structure variables is challenging in dense mixed-conifer forests on a complex terrain, since the precision of stand structure metric predictions generally decrease with increasing canopy penetration [20]. Thus, Lidar-derived forest variables have a non-negligible uncertainty associated with them.

Error is customarily defined as the difference between reality and our representation of reality [36]. When reality cannot be easily measured, error is assumed to fall within a range or distribution of possible values. There is a growing body of literature that is reporting on the ability of Lidar to predict forest structural and fuel variables [37]. However, the predicted results can be fraught with error introduced by the regression modeling process, a commonly used procedure to predict fuel metrics from Lidar measurements and field measurements, and error in these cases is evaluated using Root Mean Square Error (RMSE), which is the standard error of the regression model. Thus, in this paper, we define error as a random variable with mean of 0 and standard deviation that is equal to the calculated RMSE value derived from a regression equation describing the relationship between field-based measures and Lidar-based measures of forest structure.

There are challenges with this approach, however. It is important to note that while Lidar data is commonly evaluated in comparison to field-gathered data, there are differences in forest structure data measurements between Lidar and field-based protocols. The Lidar-derived forest structure products are created using regression models between point cloud metrics and direct measures (e.g., canopy height) or modeled estimates using allometry (e.g., canopy base height) [38]. This represents a real difference in method (i.e., regressions with direct measures vs. modeled estimates) and complicates the discussion about error in Lidar data. While acknowledging this measurement mismatch between field and Lidar data [39,40], we are using the basic error model discussed above to evaluate the influence of expected error on fire behavior results.

1.3. Error Influence on Model Results

Despite the increase in use of Lidar for mapping forests and the increasing acquisition of Lidar data over large forested areas, Lidar has not yet been routinely used to create input spatial data layers for fire behavior models. There are only a few studies that used Lidar data to create input spatial data layers for fire behavior modeling [41–44]. There are many likely reasons why this is the case [27,28,43,45–47]. Some are practical and technical, such as the complexity in Lidar processing workflow, lack of consistent Lidar data products for use in management situations, and the limited spatial extent of Lidar coverage; and, some might have to do with a lack of understanding of how accurate or useful Lidar data can be or a lack of trust of remotely sensed products by fire managers [14,15,48,49]. We know from extensive literature in spatial modeling that error associated with input spatial data layers can influence the results of a spatial modeling workflow [50–54]. While this critical body of literature does not focus on fire behavior models, the methods suggested are relevant here. One customary method to assess this influence on model result is to compute the model numerous times, with input values that are randomly sampled from a distribution of expected error using the Monte Carlo process [36].

The Monte Carlo simulation method involves specifying the probability distribution of a variable of interest (in this case Lidar error), and then performing random assignment of that variable for a specified number of runs. The method produces a distribution of results that can be compared to a model run with original data without error inclusion to evaluate the relative contribution of error on the model results. Monte Carlo simulation techniques are well suited in the field of spatial modeling, because only in rare circumstances it is possible to develop the kind of formal error analysis that is required for alternative methods. Although the Monte Carlo method requires a large number of calculations, it is attractive for its general applicability and the ease of implementation.

This paper explores the impact of error in two important Lidar-derived fire behavior model inputs—canopy height (CH) and canopy base height (CBH)—on fire behavior model results. Although

it would be useful to explicitly include the other Lidar-derived canopy structure variables (canopy cover, canopy bulk density), we chose to only examine CH and CBH for two reasons. First, these two variables represent different reasonable expectations of accuracy in Lidar data: canopy height is typically more accurately mapped using Lidar, and canopy base height is more challenging. Second, computation and analysis time for exploring all four canopy structure variables would have been prohibitive. We explored the influence of the expected variability in error on fire behavior modeling through a sensitivity analysis using a Monte Carlo simulation approach by altering the model input layers through adding randomized error and examining the results.

Specifically, our objectives were to: (1) develop landscape canopy fuels maps using Lidar data informed by a forest inventory plot network, (2) simulate landscape-level fire behavior incorporating the error that is associated with the development of canopy fuels maps (CH and CBH), and (3) estimate the relative influence of the error through mapped and statistical results. Our overall goal is to identify limits on the confidence on the output of the fire behavior modeling when such models use as input Lidar data-based layers, with some measurement error.

2. Materials and Methods

2.1. Study Area

The Last Chance study area is within the Tahoe National Forest in the northern Sierra Nevada in California, USA (Figure 1). Last Chance is a 13,767 ha site on topographically complex and steep terrain with elevation ranging from 488 to 2188 m above sea level. The climate is Mediterranean with a predominance of winter precipitation, a majority of which is snow, averaging 1182 mm per year (1990–2008; Hell Hole Remote Automated Weather Station). Most of the study area is mixed conifer forest; only 7% area is non-conifer forest (<10% of coniferous tree crown area). Dominant tree species include sugar pine (*Pinus lambertiana*), ponderosa pine (*P. ponderosa*), incense-cedar (*Calocedrus decurrens*), red and white fir (*Abies magnifica* and *A. concolor*), and California black oak (*Quercus kelloggii*). Tree densities and species composition vary with fire and management history as well as topography. From 1750 to 1900 the point fire return interval was 17.5 years, which represents the average time required for fire to re-scar the same sample within the study area; the composite fire return interval when >10% of the recording trees were scarred was 6.1 years [55]. In the 20th century, the area was subject to widespread fire suppression policies [1,56].
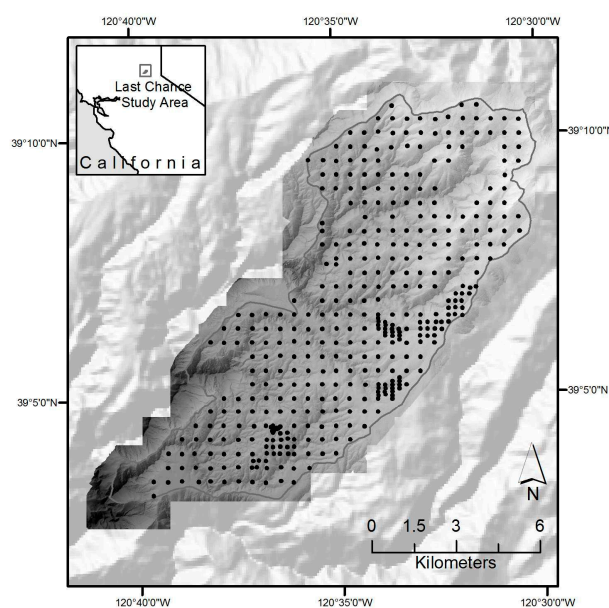

Figure 1. Last Chance Study Area in the Tahoe National Forest with field plot network.

2.2. Data Acquisition

2.2.1. Field Sampling

We systematically established forest inventory plots at 125 to 500 m spacing across the study area. Tree, shrub, canopy cover, and fuels information were collected in 0.05 ha circular plots (radius = 12.62 m) in the same year as the Lidar collection, as described in a field sampling protocol used before, and described in Collins et al. (2011) [7]. Using high precision GPS unit (Trimble[TM] GeoXH), plot center coordinates were obtained with sub-meter accuracy for 248 plots. We used summarized plot data in a regression analysis to produce the landscape forest structure and fuel model map layers for the fire behavior simulations.

2.2.2. Lidar Data

The laser scanner campaign was completed in September 2008 in five survey flights in leaf-on conditions by the National Center for Airborne Laser Mapping (NCALM) using an Optech GEMINI Airborne Laser Terrain Mapper (ALTM) sensor at an altitude of approximately 600–800 m above ground level (AGL). The Optech ALTM operated at a pulse rate frequency (PRF) of 70 KHz, with a scanning frequency of 40 Hz and a scan angle of 20°, and recorded up to four echoes per pulse. The swath width of a single pass was about 580 m. In order to increase point density the aircraft flew twice over the area with a large overlap between two adjacent swaths, such that every ground point was acquired from at least three and mostly four angles to yield an average of 9 and minimum of 6 pulses per m^2. Since the Lidar system records up to four returns per pulse, the total return density in heavy canopy forest was often greater than 10 points per m^2. The horizontal accuracy was about 10 cm and the vertical accuracy was 5.5–10 cm. From the raw point data, we developed a digital elevation model (DEM), a terrain model (DTM), and a surface model (DSM), as well as a canopy height model (CHM) at 1 m resolution [57]. We extracted from the raw Lidar point cloud the following Lidar metrics: minimum height, height percentiles (1st, 5th, 10th, 25th, 50th, 75th, 90th, 95th, and 99th), maximum, mean, standard deviations, and the coefficient of variation of height; these metrics were used with field plot data at a later step.

2.3. Fire Behavior Model Inputs

This work focuses on FlamMap, as we have experience working with this model, and have used it in the mixed conifer zone of the Sierra Nevada for several years [16,58]. FlamMap requires a standard suite of co-registered spatial data layers at the same resolution (topography (i.e., elevation, slope and aspect), canopy (i.e., canopy cover, canopy height, canopy base height, and canopy bulk density) and fuels), as well as weather data to perform simulations. Methods for these input layers are summarized in Table 1 and described here.

Table 1. Methods for generating the input layers used in FlamMap.

Spatial Layer	Development Method
Topography (Elevation, Slope, Aspect)	Created directly from interpolated Lidar last return, and resampled from 1 m DEM
Canopy Cover	Directly calculated with Lidar
Canopy Height	Regression between field plot data and Lidar metrics
Canopy Base Height	Regression between field plot data and Lidar metrics
Canopy Bulk Density	Fire and Fuels Extension in Forest Vegetation Simulator, then regression with Lidar metrics
Fuel Model	Regression between plot-measured surface fuels and Lidar metrics
Weather	Remote Automated Weather Station (RAWS)

Spatial Data Layers from Lidar. Elevation (m) was resampled to 20 m resolution from 1 m Lidar DEM using the mean values, and slope (in percent) and slope aspect (in degrees) were created from the 20-m resolution DEM. The CHM was used to create a canopy cover (CC) layer at 20-m resolution

by finding the ratio of the number of CHM pixels that fall within the pixel that have a value above a threshold (1.5 m) to the total number of CHM pixels [59]. Lidar data were processed using Python. We used plot CC, canopy bulk density (CBD), and the average of the live tree heights (CH), and heights to live crown base (CBH) as the dependent variables in a regression analysis with Lidar-derived metrics as independent variables. This approach determines the combination of coefficients that yield the best-predicted values that are correlated with the plot measured forest structure variables. The coefficients are then applied to the entire study area [27] to create four canopy fuels spatial layers.

CBD was calculated using the Fire and Fuels Extension in Forest Vegetation Simulator (FVS in [23]), with tree lists that were obtained from forest inventory plots. FVS calculates CBD, as described elsewhere [21], and assumes a uniform vertical distribution of crown fuels along the crown's length. As such, and contrary to canopy cover, our expectations were low that a predictive relationship directly with Lidar metrics could be identified and a suitable model evaluated with error in this analysis. As an alternative, we used a regression tree to assign CBD based on the same Lidar derived topographic and forest structure variables described above. Independent variables that were used included CC, CH, and elevation; model fit was moderate ($p = 0.01$, $R^2 = 0.35$), but were deemed suitable in describing forest conditions based on generalized vegetation types.

Fuel Models. To assign fuel models we developed a selection criteria utilizing fuels and shrub cover data collected from field plots. All of the fuel models used were based on Scott and Burgan [60]. Although there are other fuel classifications, some of which provide greater detail across fuel strata (e.g., Prometheus System [61], Fuel Characteristic Classification System [62], these are not currently supported in FlamMap. We used individual regression trees to predict three plot-derived fuel variables: (1) surface fuel load (includes litter and 1, 10, 100 h fuels), (2) shrub cover, (3) coarse fuel load (1000 h fuels). Independent variables that were used in the model were Lidar-derived forest structure and topographic variables: slope, aspect, elevation, canopy cover, and canopy base height. Regression trees are ideal for such an analysis because they identify break values for predictor variables that can be used to repeatedly assign fuel models to stands [7,20]. Statistical fits were moderate ($R^2 = 0.35$–0.42), but were deemed appropriate for categorizing stands into discrete fuel models. Table 2 summarizes our final fuel model selection for the entire landscape based on results from the individual regression trees. The chosen fuel models in the selection logic were based on previous studies, input from local fire/fuel managers, and on our familiarity with the study area [7,20].

Table 2. Fuel model assignments and their proportion throughout the study area. Fuel model selection logic was based on multiple regression tree analyses using plot-level data for dependent variables (shrub cover and fuel loads by category) and independent forest structure variables from Lidar data (20 m pixel resolution).

Scott and Burgan (2005) Fuel Model	Description of Stands with Fuel Model Assigned	% of Study Area
SH3 (143)	Basal Area < 50 m^2 ha^{-1}, Canopy Cover < 40%, moderate fuel load dominated by shrubs and forest litter	26
TU2 (162)	Basal Area 60 m^2 ha^{-1}, Canopy Cover > 30%, moderate fuel load dominated by shrubs and forest litter	1
TU5 (165)	Basal Area 20–80 m^2 ha^{-1}, Canopy Cover > 40%, high fuel load dominated by shrubs and forest litter	29
TL (189)	Basal Area 40–80 m^2 ha^{-1}, Canopy Cover > 30%, moderate to low site productivity	52
SB2 (202)	Basal Area > 40 m^2 ha^{-1}, Canopy Cover > 40%, high site productivity, moderate fuel load with coarse fuels present	10

Weather Data. We obtained weather information from the Duncan Peak Remote Automated Weather Station (RAWS), restricting the analysis period to the dominant fire season for the area (1 June–30 September). Observations were available from 2002 to 2009. We used 90th percentile and above wind speeds to generate multiple wind scenarios, under which fires were simulated.

We identified the dominant direction and average speed of all the observations at or above the 90th percentile value. This resulted in four different dominant wind directions, each with its own wind speed and relative frequency (based on the proportion of observations recorded at or above the 90th percentile value for each dominant direction) (Table 3). Despite incorporating multiple wind directions, we did not capture the influence of terrain on wind patterns. This choice to forego the use of more complex wind patterns, such as those output from Wind Ninja [63], was made in order to save computational and analytical time, especially given the number of simulations employed (described below). We used 95th percentile fuel moistures, which combined with the filtered wind speeds, capture conditions that are associated with large wildfire growth. As a result, our modeled fires represent only those fires that are likely to escape initial fire suppression efforts.

Table 3. Parameters used for fire behavior model simulations. Parameters were drawn from the Duncan Remote Automated Weather Station, and represent the 90th percentile and above winds and the 95th percentile fuel moistures for the predominant fire season in the area (1 June–30 September).

Weather Input	Specific Parameter/Value				
	Speed (km/h)		Direction (Degrees az.)		Relative Frequency
Wind	19		225		0.75
	20		45		0.10
	19		180		0.05
Fuel Type	1 h	10 h	100 h	Live Herbaceous	Live Woody
Moisture Content (%)	2	3	5	30	60

2.4. Fire Behavior Model Simulations

We employed a command-line version of FlamMap [19], called RANDIG, to model fires across the Last Chance landscape. FlamMap uses the minimum travel time (MTT) algorithm [64] to simulate fire spread based on Huygens' Principle, where the growth and behavior of a fire edge is modeled as a vector or wave front [64,65]. Fire spread is predicted by the Rothermel equations [66], and crown fire initiation is evaluated according theory for start and spread of crown fire presented by Van Wagner [67], and as implemented by Scott and Reinhardt [21]. Extensive application has demonstrated that the Huygens' principle in general, and the MTT algorithm in particular, can predict fire spread and replicate large fire boundaries in heterogeneous ecosystems reasonably well [12,68–75].

In addition to landscape topographic and canopy fuels maps described above, RANDIG requires the number/pattern of ignitions, fire duration, wind speed and direction, and fuel moistures. For each fire behavior model run, we simulated 10,000 randomly placed ignitions, burning for 240 min. While the use of numerous randomly place ignitions is not a true application of a Monte Carlo method, the intent with it is to remove the influence of fire start location as a significant influence on the model outputs. The burn period duration was selected, such that simulated fire sizes (for one burn period) approximated large spread events (daily) observed in actual fires that occurred near the study area [13]. There were three recent fires that burned near or within the Last Chance study area, for which daily spread information existed: the 2001 Star Fire, the 2008 American River Fire complex, and the 2013 American Fire. The range of average simulated fire sizes for our experimental runs (1500–2100 ha) approximates the largest daily spread events that were observed in these three fires. However, a nearby wildfire, the 2014 King Fire, demonstrated extreme fire growth that was an order of magnitude larger than our modeled daily spread events. This emphasizes a limitation of our modeling approach in that it is not capturing the extreme plume-dominated fire growth [76]. Instead, our approach likely represents larger (albeit not extreme) wind-driven fire events in Sierra Nevada mixed-conifer forests.

All data layers were combined with a grid cell resolution of 20 m, maintaining the detail of the canopy surface models. Outputs from FlamMap include: (1) mapped conditional burn probability (CBP), (2) and a collection of 20 mapped marginal conditional burn probabilities (CBPi) from 0–10 m

parsed into 0.5 m flame length classes at 40 m resolution, and (3) mapped modeled fires, one fire per run. Conditional burn probabilities are computed by dividing the total number of times a pixel burned by the total number of simulated fires (10,000 random ignitions). The conditional burn probability for a given pixel is an estimate of the likelihood that a pixel with the given forest and environmental conditions will burn given a single random ignition. To identify more problematic simulated fire occurrences we performed analysis on the burn probabilities for which modeled flame lengths were greater than the critical flame length, where the potential for crown fire initiation is high. The CBPi outputs were used to calculate the probabilities with flame lengths greater than the critical flame length set to 2 m by summing CBPi outputs of value greater than 2 m (i.e., 2 m + 2.5 m + 3 m, etc.).

2.4.1. Monte Carlo Simulations

We used a Monte Carlo simulation analysis focusing on two canopy fuels variables—CH and CBH—in our simulation experiment. We ran the FlamMap simulation to generate conditional burn probability based on the original set of eight topographic, canopy fuels, and surface fuel model layers. We simulated error propagation by generating the same conditional burn probability estimates for two additional scenarios, with 100 runs each. This resulted in a total of 201 different conditional burn probability surfaces. We chose to run the model 100 times (and not more, as is typical with Monte Carlo simulations), as there is to date no scripted version of the model, and each run took considerable computation and analyst time. Model 1 used the original, unmodified data; Model 2 used 100 versions of the perturbed CH layer (CH + Error), and Model 3 used 100 versions of the perturbed CBH layer (CBH + Error). The workflow for Model 2 (CH + Error) is shown in Figure 2, and the workflow also applies to Model 3 (CBH + Error). In each case, the 100 error estimates for CH and CBH were generated through random sampling from a Gaussian distribution, with mean = 0 and standard deviation being equal to the calculated RMSE value that was derived from each regression equation and added to the original CH or CBH values.
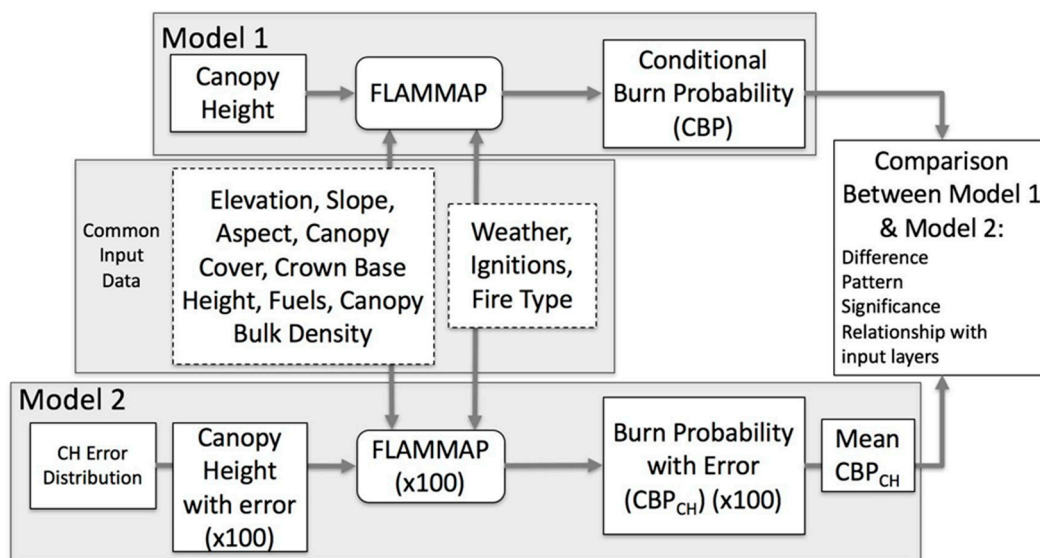

Figure 2. General workflow for creating original Model 1 run with original data, and Model 2 run (Monte Carlo with Canopy Height + Error). The same workflow holds for Model Scenario 3 (Crown Base Height + Error).

2.4.2. Evaluation of Error Impact on Model Result

Comparisons between Model 1 (original data) and Models 2 and 3 allow for the interpretation of the changes in modeled fire behavior that is caused by measurement error. For each CBP result, we selected fires of flame lengths >2 m (corresponding to crown fire initiation and more problematic

fire occurrence from a fire suppression and modeling perspective) for the subsequent analysis. First, we calculated the difference between the original CBP (Model 1) and the individual error CBP maps for Models 2 and 3. We compared the distribution of fire size classes between all of the models, and compared how fire size related to number of ignitions across all the models.

To test the significance of the difference between the original run and the runs with error, we calculated a *z*-score for Model 2 and Model 3, according to the formula:

$$Z = (\frac{(Obs - Exp)}{\sigma Obs})$$

where *Obs* is the result from Model 2 or Model 3, *Exp* is the result from Model 1, and σ is the standard deviation. These *z*-scores were compared to canopy height and canopy base height and other model input layers through regression. We divided each variable into a set number of bins based on a constant interval (e.g., 5 m for CH, 5% for CC, 0.2 m for CBH, 100 m for elevation, 5° for slope, and 30° for aspect). *Z*-scores for Model 2 or Model 3 were regrouped based on the divided bins of each factor, and the mean difference for each bin was calculated. Regression analysis was used to reveal how different input factors influenced the differences between simulation results. Linear regression, polynomial regression, and piecewise linear regression were tested, respectively, to get the best fit for each analysis.

3. Results

3.1. Canopy Height and Canopy Base Height

Forest structural characteristics in the Last Chance study area are typical of Sierra Nevada mixed conifer forests. Results from the regression equations used to create CH and CBH layers are shown in Table 4. CH was best modeled using the mean and 25th percentile Lidar metrics as important predictors ($p < 0.0001$, $R^2 = 0.81$). CBH was best modeled using the 10th and 25th percentile Lidar metrics ($p < 0.0001$, $R^2 = 0.51$). Both regression equations were significant. The RMSE of 4.12 m (CH) and 1.62 m (CBH) were used to develop 100 perturbed layers with introduced error for both CH and CBH, as described in the Methods section above.

Table 4. Details of canopy height and crown base height field data, and details of resulting regression with Lidar metrics.

Forest Variables	Mean (SD)	Minimum-Maximum	Regression Equation	R^2 (RMSE)
Canopy Height (m)	23.3 (10.1)	0–51.9	$4.73 - 0.82 \times L25th + 1.88 \times L_{mean}$	0.81 (4.12 m)
Crown base height (m)	3.7 (2.4)	0–12.7	$0.17 + 0.25 \times L10th + 0.30 \times L25th$	0.51 (1.62 m)

SD = Standard Deviation of the Mean; L_{mean} = Mean of Lidar returns; L25th = 25th percentile of Lidar returns; L10th = 10th percentile of Lidar returns.

3.2. Fire Behavior Model Results

The conditional burn probability of the study area is depicted in Figure 3. Some areas are more likely to burn and they are shown in red versus other areas that burn less often, which are shown in green. The conditional burn probabilities that are produced from Model 1 with the original data ranged from 0.0 to 0.225, with a mean of 0.049. This overall pattern of CBP did not change when CH and CBH error were included in the simulation. Model 2 (CH + Error) ranged from 0.0 to 0.220, with a mean of 0.048 and Model 3 (CBH + Error), ranged from 0.0 to 0.193, with a mean of 0.049 (Figure 3).
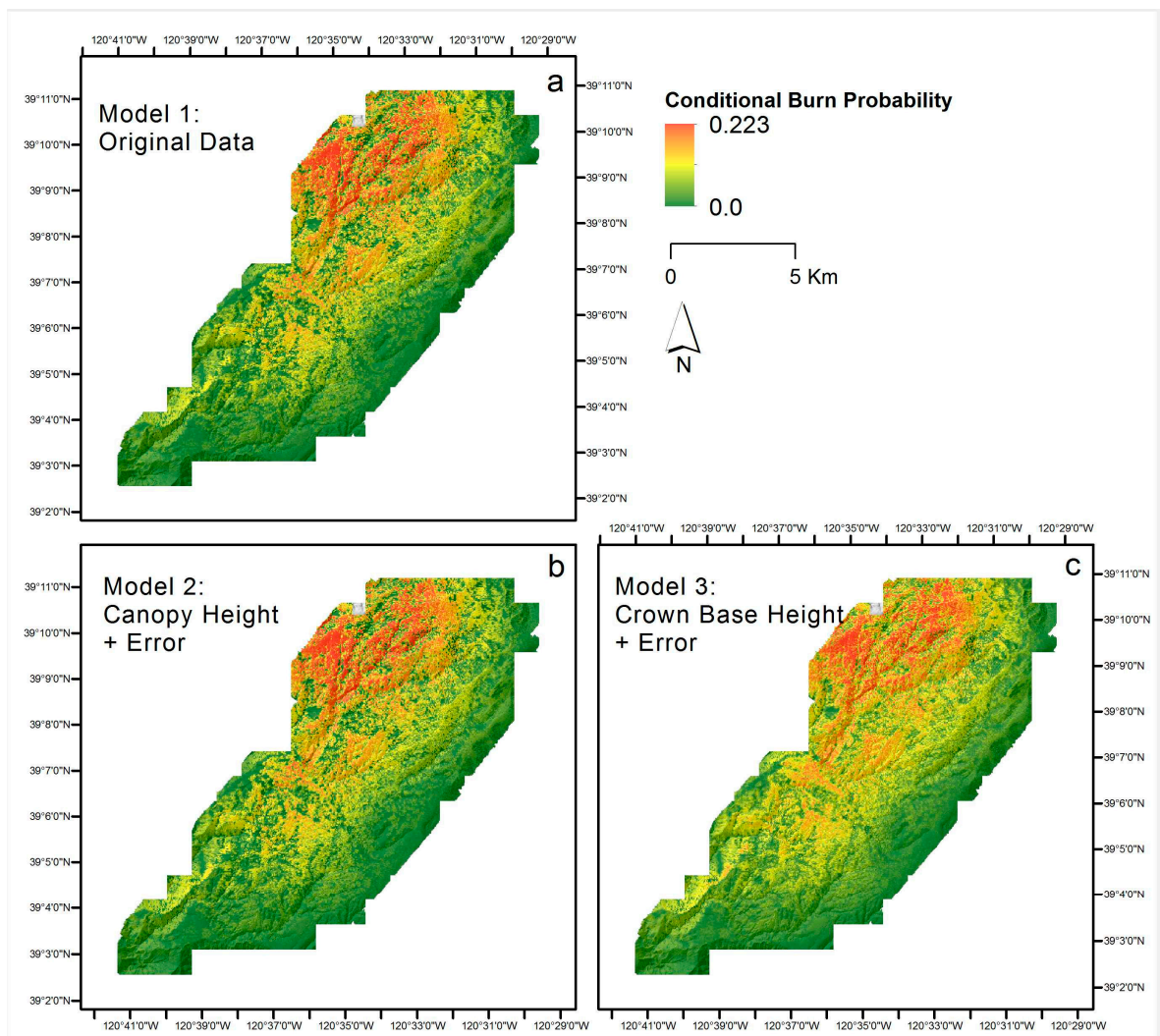
Figure 3. Map of conditional burn probability (CBP) for high severity fires across the Last Chance study area (40 m resolution): (**a**) Model 1 (original data); (**b**) Average CBP for 100 runs of Model 2 (CH + Error); and, (**c**) Average CBP for 100 runs of Model 3 (CBH + Error).

The difference between Model 1 and Model 2 was slight, and ranged from −0.055 to 0.007. CPB increases were apparent on the margins of the study area, and largest decreases in the central study area, areas with higher CC and elevation. The difference between Model 1 and Model 3 was larger, and ranged from −0.122 to 0.116 (Figure 4). Increases in CBP were apparent across the study area and decreases were apparent mainly in the northwest.
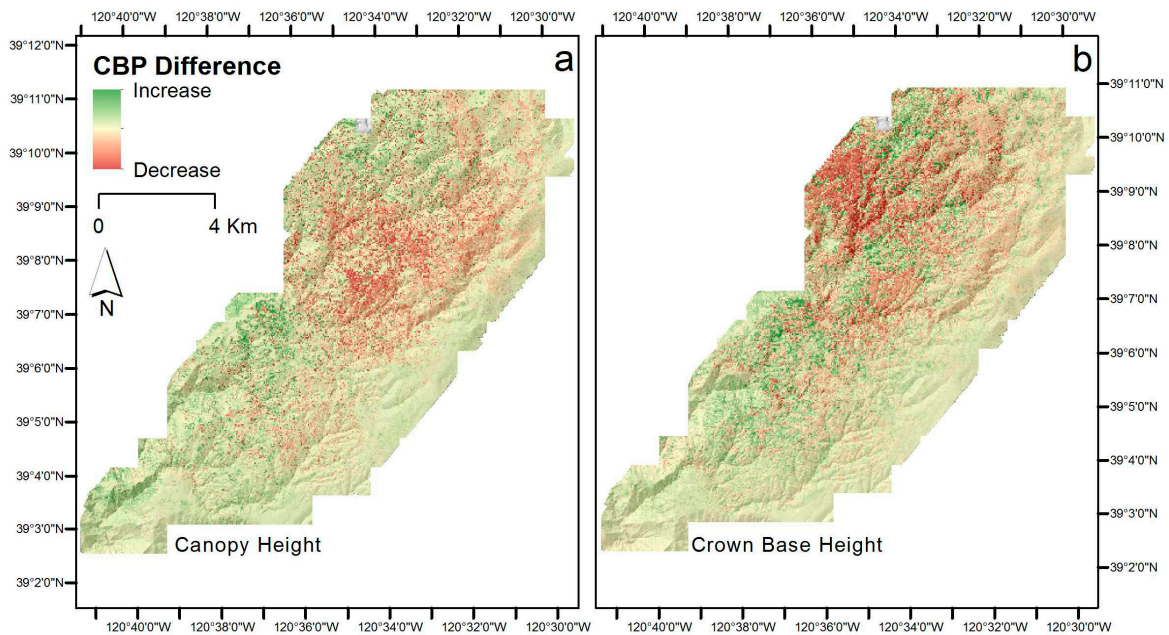
Figure 4. Difference in modeled conditional burn probability for (**a**) Model 2 (Canopy Height + Error) minus Model 1 (original data), and (**b**) Model 3 (Canopy Base Height + Error) minus Model 1 (original data).

A distribution of modeled area of CBP for each Model reveals little error impact, with only slight differences in Model 3 at low and high CBP (Figure 5a). Fire size differences between models are consistent with this. The mean fire size in Model 1 was 1313.0 ha (SD = 822.32 ha) and ranged from 0.3 to 4328.5 ha. For Model 2, the mean fire size was 1295.2 ha, and ranged from 0.3 to 4430.9 ha, and for Model 3, the mean was 1277.3 ha, and it ranged from 0.32 to 4115.5 ha. Fire size distributions with respect to the number of ignitions for Model 2 and Model 3 were similar to Model 1 (Figure 5b).
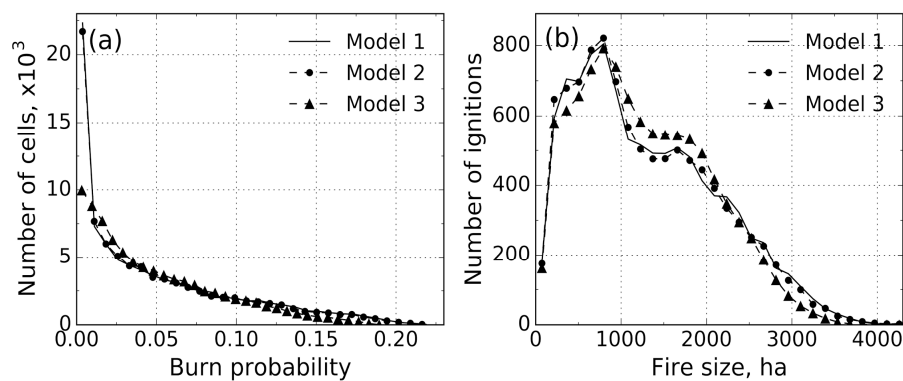

Figure 5. Distribution of (**a**) conditional burn probability, and (**b**) fire size for Model 1, Model 2, and Model 3. Note that the conditional burn probability shown for Model 2 and Model 3 is the average of 100 runs, and the number of ignitions is the average frequency of the 100 runs within each fire size bin.

3.3. Relationship Between Significant Difference in CBP and Model Input Variables

There were strong and predictable relationships between the significant difference in modeled CBP (*z*-score) and CH and CBH. There were moderate fits between CC and *z*-score value ($R^2 = 0.63$), and CBH and *z*-score value ($R^2 = 0.49$) in Model 2. At lower canopy heights, the addition of error from the CH data layer (Model 2) increased CBP (values above the 0.0 line in Figure 6a), and this trend was similar for CBH (Figure 6b), with higher canopy base height decreasing modeled CBD. In Model 3,

there were good fits between CC and *z*-score value ($R^2 = 0.79$) and moderate fit between CBH and *z*-score value ($R^2 = 0.56$). Similar to with Model 2, at lower canopy heights, the addition of error from canopy base height data layer (Model 3) increased CBP (Figure 7a), and increases in CBH lessened the modeled CBP (Figure 7b).
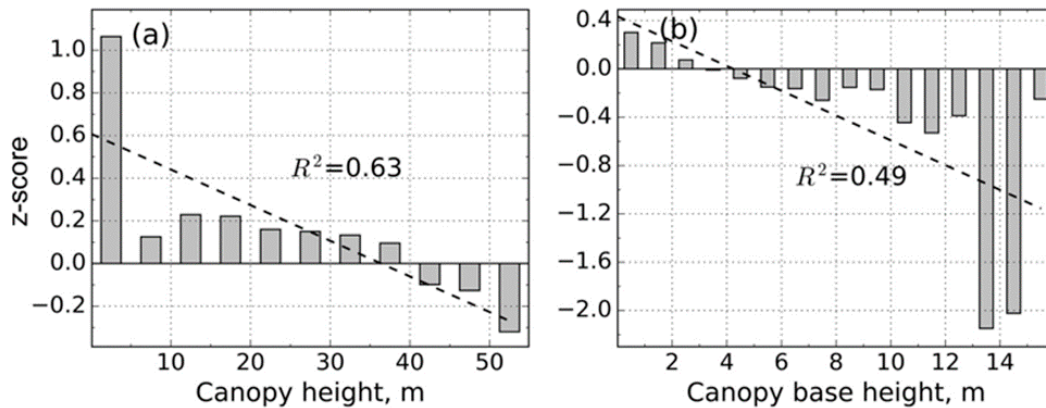

Figure 6. Relationship between *z*-score (significant differences) in modeled CBP between Model 1 and Model 2 (Canopy Height + Error) and (**a**) canopy height, and (**b**) canopy base height.
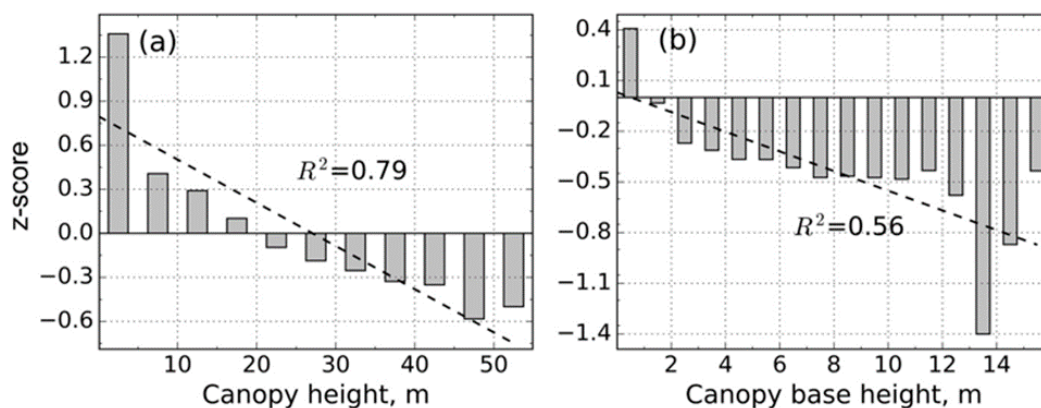

Figure 7. Relationship between *z*-score (significant differences) in modeled CBP between Model 1 and Model 3 (Canopy Base Height + Error) and (**a**) canopy height, and (**b**) canopy base height.

4. Discussion

There is considerable uncertainty in spatially explicit fire behavior modeling. Much of this uncertainty is the result of inherent variability in forest structure and surface fuels at multiple spatial scales [77]. Developing spatially comprehensive products that are based on interpolating information from discrete field plots may not robustly capture this variability, especially in complex forests. Error in input spatial products when captured from field data is rarely reported or estimated, and overall uncertainties that these data create are rarely addressed in the literature describing operational fire behavior modeling [6,7]. These errors can include errors in forest structure inputs, as well as errors in fuel model estimation, which can be very large [20]. In contrast, analysts produce wall-to-wall detailed maps of forest structure from Lidar data that can be compared to field measures in order to derive error measures [20,27–29,45,47]. As noted earlier, there can be a measurement mismatch between Lidar and field-based data protocols, in particular with CBH. CBH—or the height above which there is sufficient fuel to move a fire upward—is a critical component for assessing fire hazard in a given area [38,78,79] yet it is difficult to measure. Lidar-derived CBH involves regressions between point cloud metrics and plot data [20,27–29,49], while the typical measurement for CBH without Lidar

involves estimates at the plot scale through allometric equations that consider species, diameter at breast height (DBH), tree height, crown length, height to live crown base, crown ratio, and crown width [38,78,79]. This discrepancy in method (i.e., regression with direct measures vs. modeled estimate) can result in a low correlation between Lidar and field estimates for CBH [20,35,79], and thus inflating the error estimates that are associated with CBH.

Our work showed that the impact on modeled results of expected errors associated with Lidar-based forest structure are not significant. Conditional burn probability, fire size, and fire size distributions were very similar between models run with and without added error. However, there are important aspects that need further discussion. First, the impact of introduced error is more pronounced when the error is introduced to the CBH layer than with the CH layer (e.g., the difference between modeled CBP in the former (CBH) case is -0.1217 to 0.1157, as compared to -0.0547 to 0.0065 in the latter (CH) case). This is not surprising, as the CBH error is larger proportionally than the CH error. Second, the introduction of error in both CH and CBH layers at lower CBHs serves to increase modeled CBP. This is a logical result when one considers how influential CBH is on hazardous fire potential [8]. Fire propagation in forested environments is strongly influenced by the transition from surface fire to crown fire [21,80]. Ladder fuels, or forest fuels that provide vertical fuel continuity and can preheat canopy fuels that have not yet ignited [38,79,81] are important in fire behavior, but US fire behavior models such as FlamMap and Farsite are not currently able to use a quantitative measure of ladder fuels in forests. Instead, CBH is used in US fire behavior models to represent the vertical fuel structure in forests. CBH is used in increments of 0.5 m in spatial fire behavior models that can be used on large area, such as the Last Chance study area.

Our results focused on two extremes of Lidar error—canopy height is easiest to measure with Lidar and canopy base height is more difficult—but we need to also consider how error in the other input layers—topography, canopy cover, crown bulk density, and surface fuels—can influence the modeled results. While Lidar-derived topographic variables are generally considered accurate [57], crown bulk density and surface fuels are very difficult to capture accurately over large areas with field methods or with Lidar [20]. Further exploration is needed that examines the contributions to uncertainty from each of the input layers that are used in models such as FlamMap.

It is well documented elsewhere [20] that the accuracy of products that are derived from discrete return Lidar captured from an aircraft decreases with increased penetration into dense forest canopy. New technological developments will likely ameliorate this. For example, there is an expectation that full waveform Lidar will produce more detailed characterizations of vegetation structure, due to its ability to digitize and record the entire backscattered signal of each laser pulse [82,83]. Studies focusing on canopy bulk density and CBH estimation using large-footprint, waveform-digitizing Lidar data have reported good results (e.g., [84]), demonstrating that waveform data from a large-footprint system may provide the spatially explicit forest structure that is needed for fire behavior modeling. Additionally, developments in mobile ground based Lidar (e.g., portable canopy Lidar or portable profiling Lidar) will likely be able to map important inter-canopy forest structure variables [85,86] in more detail. Moreover, new methods to link novel ground measurements of critical forest structure—such as presence and condition of ladder fuels—will likely prove fruitful [38].

One of the key uses for fire behavior models is to explore the impacts of fuel treatment alternatives across forested landscapes [87]. While we did not explicitly examine the interaction between error and potential fuel treatment location, there is little here to suggest that the error introduced by Lidar data would significantly influence any modeled treatment impact. This is perhaps useful information for forest and fire managers, who are tasked with planning landscape level forest fuel treatments, exploring fuel treatment alternatives across land ownerships, and using fire behavior models to contribute to the planning process that is mandated for the management of federal and state agencies [6,7].

5. Conclusions

Lidar data is increasingly being used in operational forest management to quantify and map forest characteristics [45,88,89], and it is being acquired across increasingly large forest landscapes. Lidar data products will likely be increasingly used in fire behavior models as increasing numbers of forest managers acquire these data. However, they are not yet routinely used in fire behavior modeling. The challenge is not that Lidar-based estimates of CH and CBH have errors, they do (as do field-based estimates). But rather, that forest fire managers are used to dealing fire behavior models when critical inputs are estimated from field measurements. Managers need an assessment of how their fire behavior models will operate differently when parameters such as CH and CBH are estimated from Lidar measurements instead of field measurements. Here, we investigated the influence of error in Lidar-derived CH and CBH on fire behavior models through a Monte Carlo sensitivity analysis in a case study area in the Sierra Nevada in California. We developed three models (Model 1 used the original, unmodified data, Model 2 incorporated error in the CH layer, and Model 3 incorporated error in the CBH layer) and examined the difference, pattern, and significance of conditional burn probability and fire size, and the relationship between significant areas of change with other model input layers. We found that the expected error that is associated with CH and CBH did not greatly influence modeled results: conditional burn probability, fire size, and fire size distributions were very similar between Model 1 (original data), Model 2 (error added to CH), and Model 3 (error added to CBH). Important lessons include: (1) the impact of introduced error is more pronounced with CBH than with CH; and, (2) at lower canopy heights, the addition of error increased modeled canopy burn probability.

As Lidar data is more commonly collected for forests, a better understanding of the influence of Lidar-derived layer error on the fire behavior modeling process might help forest managers and scientists to better evaluate how Lidar can play a role in their work. Our work suggests that the use of Lidar data, even with its inherent error, can contribute to reliable and robust estimates of modeled forest fire behavior and forest managers should be confident in using Lidar data products in their fire behavior modeling workflow.

Author Contributions: Maggi Kelly, Qinghua Guo and Scott L. Stephens conceived and designed the experiment; Brandon Collins and Danny Fry performed the fire behavior modeling; Maggi Kelly, Yanjun Su and Stefania Di Tommaso analyzed the data; Maggi Kelly and Yanjun Su wrote the paper. Maggi Kelly, Scott L. Stephens, Qinghua Guo and Yanjun Su revised the manuscript.

References

1.　Stephens, S.L.; Collins, B.M.; Biber, E.; Fulé, P.Z. US federal fire and forest policy: Emphasizing resilience in dry forests. *Ecosphere* **2016**, *7*. [CrossRef]

2.　Hessburg, P.F.; Churchill, D.J.; Larson, A.J.; Haugo, R.D.; Miller, C.; Spies, T.A.; North, M.P.; Povak, N.A.; Belote, R.T.; Singleton, P.H. Others Restoring fire-prone Inland Pacific landscapes: Seven core principles. *Landsc. Ecol.* **2015**, *30*, 1805–1835. [CrossRef]

3.　Williams, A.P.; Allen, C.D.; Millar, C.I.; Swetnam, T.W.; Michaelsen, J.; Still, C.J.; Leavitt, S.W. Forest responses to increasing aridity and warmth in the southwestern United States. *Proc. Natl. Acad. Sci. USA* **2010**, *107*, 21289–21294. [CrossRef] [PubMed]

4. Allen, C.D. Interactions across Spatial Scales among Forest Dieback, Fire, and Erosion in Northern New Mexico Landscapes. *Ecosystems* **2007**, *10*, 797–808. [CrossRef]

5. Williams, A.P.; Seager, R.; Berkelhammer, M.; Macalady, A.K.; Crimmins, M.A.; Swetnam, T.W.; Trugman, A.T.; Buenning, N.; Hryniw, N.; McDowell, N.G.; et al. Causes and Implications of Extreme Atmospheric Moisture Demand during the Record-Breaking 2011 Wildfire Season in the Southwestern United States. *J. Appl. Meteorol. Climatol.* **2014**, *53*, 2671–2684. [CrossRef]

6. Collins, B.M.; Stephens, S.L.; Moghaddas, J.J.; Battles, J. Challenges and approaches in planning fuel treatments across fire-excluded forested landscapes. *J. For.* **2010**, *108*, 24–31.

7. Collins, B.M.; Stephens, S.L.; Roller, G.B.; Battles, J.J. Simulating fire and forest dynamics for a landscape fuel treatment project in the Sierra Nevada. *For. Sci.* **2011**, *57*, 77–88.

8. Collins, B.M.; Kramer, H.A.; Menning, K.; Dillingham, C.; Saah, D.; Stine, P.A.; Stephens, S.L. Modeling hazardous fire potential within a completed fuel treatment network in the northern Sierra Nevada. *For. Ecol. Manag.* **2013**, *310*, 156–166. [CrossRef]

9. Miller, C.; Ager, A.A. A review of recent advances in risk analysis for wildfire management. *Int. J. Wildland Fire* **2013**, *22*, 1–14. [CrossRef]

10. Moghaddas, J.J.; Collins, B.M.; Menning, K.; Moghaddas, E.E.Y.; Stephens, S.L. Fuel treatment effects on modeled landscape-level fire behavior in the northern Sierra Nevada. *Can. J. For. Res.* **2010**, *40*, 1751–1765. [CrossRef]

11. Hollingsworth, L.T.; Kurth, L.L.; Parresol, B.R.; Ottmar, R.D.; Prichard, S.J. A comparison of geospatially modeled fire behavior and fire management utility of three data sources in the southeastern United States. *For. Ecol. Manag.* **2012**, *273*, 43–49. [CrossRef]

12. Ager, A.A.; Finney, M.A.; Kerns, B.K.; Maffei, H. Modeling wildfire risk to northern spotted owl (*Strix occidentalis caurina*) habitat in Central Oregon, USA. *For. Ecol. Manag.* **2007**, *246*, 45–56. [CrossRef]

13. Ager, A.A.; Vaillant, N.M.; Finney, M.A. A comparison of landscape fuel treatment strategies to mitigate wildland fire risk in the urban interface and preserve old forest structure. *For. Ecol. Manag.* **2010**, *259*, 1556–1570. [CrossRef]

14. Keane, R.E.; Burgan, R.; van Wagtendonk, J. Mapping wildland fuels for fire management across multiple scales: Integrating remote sensing, GIS, and biophysical modeling. *Int. J. Wildland Fire* **2001**, *10*, 301–319. [CrossRef]

15. Keane, R.E.; Reeves, M. Use of Expert Knowledge to Develop Fuel Maps for Wildland Fire Management. In *Expert Knowledge and Its Application in Landscape Ecology*; Springer: New York, NY, USA, 2012; pp. 211–228, ISBN 9781461410331.

16. Krasnow, K.D.; Fry, D.L.; Stephens, S.L. Spatial, temporal and latitudinal components of historical fire regimes in mixed conifer forests, California. *J. Biogeogr.* **2017**, *44*, 1239–1253. [CrossRef]

17. Burgan, R.E.; Rothermel, R.C. *Authors BEHAVE: Fire Behavior Prediction and Fuel Modeling System—FUEL Subsystem*; USDA Forest Service: Washington, DC, USA, 1984.

18. Finney, M.A. *FARSITE, Fire Area Simulator—Model Development and Evaluation*; U.S. Department of Agriculture, Forest Service, Rocky Mountain Research Station: Fort Collins, CO, USA, 1998; Volume 3.

19. Finney, M.A. An overview of FlamMap fire modeling capabilities. In *Fuels Management—How to Measure Success*; U.S. Department of Agriculture, Forest Service, Rocky Mountain Research Station: Fort Collins, CO, USA, 2006; pp. 213–220.

20. Jakubowski, M.K.; Guo, Q.; Collins, B.; Stephens, S.; Kelly, M. Predicting Surface Fuel Models and Fuel Metrics Using Lidar and CIR Imagery in a Dense, Mountainous Forest. *Photogramm. Eng. Remote Sens.* **2013**, *79*, 37–49. [CrossRef]

21. Scott, J.H.; Reinhardt, E.D. Assessing crown fire potential by linking models of surface and crown fire behavior. In *USDA Forest Service Research Note*; U.S. Department of Agriculture, Forest Service, Rocky Mountain Research Station: Fort Collins, CO, USA, 2001; p. 1.

22. Hall, S.A.; Burke, I.C. Considerations for characterizing fuels as inputs for fire behavior models. *For. Ecol. Manag.* **2006**, *227*, 102–114. [CrossRef]

23. Reinhardt, E.D.; Crookston, N.L. *The Fire and Fuels Extension to the Forest Vegetation Simulator*; U.S. Department of Agriculture, Forest Service, Rocky Mountain Research Station: Colorado, CO, USA, 2003.

24. Van Wagner, C.E. Prediction of crown fire behavior in two stands of jack pine. *Can. J. For. Res.* **1993**, *23*, 442–449. [CrossRef]

25. Sando, R.W.; Wick, C.H. *A Method of Evaluating Crown Fuels in Forest Stands*; U.S. Department of Agriculture, Forest Service, Rocky Mountain Research Station: Fort Collins, CO, USA, 1972.

26. Schmidt, D.A.; Taylor, A.H.; Skinner, C.N. The influence of fuels treatment and landscape arrangement on simulated fire behavior, Southern Cascade range, California. *For. Ecol. Manag.* **2008**, *255*, 3170–3184. [CrossRef]

27. Andersen, H.-E.; McGaughey, R.J.; Reutebuch, S.E. Estimating forest canopy fuel parameters using LIDAR data. *Remote Sens. Environ.* **2005**, *94*, 441–449. [CrossRef]

28. Kelly, M.; Di Tommaso, S. Mapping forests with Lidar provides flexible, accurate data with many uses. *Calif. Agric.* **2015**, *69*, 14–20. [CrossRef]

29. Zhao, F.; Guo, Q.; Kelly, M. Allometric equation choice impacts lidar-based forest biomass estimates: A case study from the Sierra National Forest, CA. *Agric. For. Meteorol.* **2012**, *165*, 64–72. [CrossRef]

30. Su, Y.; Ma, Q.; Guo, Q. Fine-resolution forest tree height estimation across the Sierra Nevada through the integration of spaceborne LiDAR, airborne LiDAR, and optical imagery. *Int. J. Digit. Earth* **2017**, *10*, 307–323. [CrossRef]

31. Su, Y.; Guo, Q.; Collins, B.M.; Fry, D.L.; Hu, T.; Kelly, M. Forest fuel treatment detection using multi-temporal airborne lidar data and high-resolution aerial imagery: A case study in the Sierra Nevada Mountains, California. *Int. J. Remote Sens.* **2016**, *37*, 3322–3345. [CrossRef]

32. Su, Y.; Guo, Q.; Fry, D.L.; Collins, B.M.; Kelly, M.; Flanagan, J.P.; Battles, J.J. A Vegetation Mapping Strategy for Conifer Forests by Combining Airborne LiDAR Data and Aerial Imagery. *Can. J. Remote Sens.* **2016**, *42*, 1–15. [CrossRef]

33. McRoberts, R.E.; Næsset, E.; Gobakken, T. Inference for lidar-assisted estimation of forest growing stock volume. *Remote Sens. Environ.* **2013**, *128*, 268–275. [CrossRef]

34. Hyde, P.; Dubayah, R.; Peterson, B.; Blair, J.B.; Hofton, M.; Hunsaker, C.; Knox, R.; Walker, W. Mapping forest structure for wildlife habitat analysis using waveform lidar: Validation of montane ecosystems. *Remote Sens. Environ.* **2005**, *96*, 427–437. [CrossRef]

35. Erdody, T.L.; Moskal, L.M. Fusion of LiDAR and imagery for estimating forest canopy fuels. *Remote Sens. Environ.* **2010**, *114*, 725–737. [CrossRef]

36. Heuvelink, G.B.M. *Error Propagation in Environmental Modelling with GIS*; CRC Press: Boca Raton, FL, USA, 1998; ISBN 9780748407446.

37. White, J.C.; Coops, N.C.; Wulder, M.A.; Vastaranta, M.; Hilker, T.; Tompalski, P. Remote Sensing Technologies for Enhancing Forest Inventories: A Review. *Can. J. Remote Sens.* **2016**, *42*, 619–641. [CrossRef]

38. Kramer, H.; Collins, B.; Lake, F.; Jakubowski, M.; Stephens, S.; Kelly, M. Estimating Ladder Fuels: A New Approach Combining Field Photography with LiDAR. *Remote Sens.* **2016**, *8*, 766. [CrossRef]

39. Ferraz, A.; Saatchi, S.; Mallet, C.; Jacquemoud, S.; Gonçalves, G.; Silva, C.A.; Soares, P.; Tomé, M.; Pereira, L. Airborne Lidar Estimation of Aboveground Forest Biomass in the Absence of Field Inventory. *Remote Sens.* **2016**, *8*, 653. [CrossRef]

40. González-Ferreiro, E.; Arellano-Pérez, S.; Castedo-Dorado, F.; Hevia, A.; Vega, J.A.; Vega-Nieva, D.; Álvarez-González, J.G.; Ruiz-González, A.D. Modelling the vertical distribution of canopy fuel load using national forest inventory and low-density airbone laser scanning data. *PLoS ONE* **2017**, *12*, e0176114. [CrossRef] [PubMed]

41. Riano, D.; Meier, E.; Allgöwer, B.; Chuvieco, E.; Ustin, S.L. Modeling airborne laser scanning data for the spatial generation of critical forest parameters in fire behavior modeling. *Remote Sens. Environ.* **2003**, *86*, 177–186. [CrossRef]

42. González-Olabarria, J.-R.; Rodríguez, F.; Fernández-Landa, A.; Mola-Yudego, B. Mapping fire risk in the Model Forest of Urbión (Spain) based on airborne LiDAR measurements. *For. Ecol. Manag.* **2012**, *282*, 149–156. [CrossRef]

43. Mutlu, M.; Popescu, S.C.; Zhao, K. Sensitivity analysis of fire behavior modeling with LIDAR-derived surface fuel maps. *For. Ecol. Manag.* **2008**, *256*, 289–294. [CrossRef]

44. Mutlu, M.; Popescu, S.C.; Stripling, C.; Spencer, T. Mapping surface fuel models using lidar and multispectral data fusion for fire behavior. *Remote Sens. Environ.* **2008**, *112*, 274–285. [CrossRef]

45. Wulder, M.A.; Bater, C.W.; Coops, N.C.; Hilker, T.; White, J.C. The role of LiDAR in sustainable forest management. *For. Chron.* **2008**, *84*, 807–826. [CrossRef]

46. Akay, A.E.; Oğuz, H.; Karas, I.R.; Aruga, K. Using LiDAR technology in forestry activities. *Environ. Monit. Assess.* **2009**, *151*, 117–125. [CrossRef] [PubMed]

47. Jakubowski, M.K.; Guo, Q.; Kelly, M. Tradeoffs between lidar pulse density and forest measurement accuracy. *Remote Sens. Environ.* **2013**, *130*, 245–253. [CrossRef]

48. Butterfield, H.S.; Malmstrom, C.M. Experimental Use of Remote Sensing by Private Range Managers and Its Influence on Management Decisions. *Rangel. Ecol. Manag.* **2006**, *59*, 541–548. [CrossRef]

49. Trigg, S.N.; Roy, D.P. A focus group study of factors that promote and constrain the use of satellite-derived fire products by resource managers in southern Africa. *J. Environ. Manag.* **2007**, *82*, 95–110. [CrossRef] [PubMed]

50. Heuvelink, G.B.M.; Burrough, P.A. Error propagation in cartographic modelling using Boolean logic and continuous classification. *Int. J. Geogr. Inf. Syst.* **1993**, *7*, 231–246. [CrossRef]

51. Heuvelink, G.B.M.; Burrough, P.A.; Stein, A. Propagation of errors in spatial modelling with GIS. *Int. J. Geogr. Inf. Syst.* **1989**, *3*, 303–322. [CrossRef]

52. Crosetto, M.; Tarantola, S.; Saltelli, A. Sensitivity and uncertainty analysis in spatial modelling based on GIS. *Agric. Ecosyst. Environ.* **2000**, *81*, 71–79. [CrossRef]

53. Goodchild, M.F. Integrating GIS and remote sensing for vegetation analysis and modeling: Methodological issues. *J. Veg. Sci.* **1994**, *5*, 615–626. [CrossRef]

54. Goodchild, M.F.; Gopal, S. *The Accuracy of Spatial Databases*; CRC Press: Boca Raton, FL, USA, 1989; ISBN 9780203490235.

55. Stephens, S.L.; Collins, B.M. Fire regimes of mixed conifer forests in the north-central Sierra Nevada at multiple spatial scales. *Northwest Sci.* **2004**, *78*, 12–23.

56. Stephens, S.L.; Ruth, L.W. Federal Forest-Fire Policy in the United States. *Ecol. Appl.* **2005**, *15*, 532–542. [CrossRef]

57. Guo, Q.; Li, W.; Yu, H.; Alvarez, O. Effects of topographic variability and lidar sampling density on several DEM interpolation methods. *Photogramm. Eng. Remote Sens.* **2010**, *76*, 701–712. [CrossRef]

58. Collins, B.M.; Stevens, J.T.; Miller, J.D.; Stephens, S.L.; Brown, P.M.; North, M.P. Alternative characterization of forest fire regimes: Incorporating spatial patterns. *Landsc. Ecol.* **2017**, 1–10. [CrossRef]

59. Lucas, R.M.; Cronin, N.; Lee, A.; Moghaddam, M.; Witte, C.; Tickle, P. Empirical relationships between AIRSAR backscatter and LiDAR-derived forest biomass, Queensland, Australia. *Remote Sens. Environ.* **2006**, *100*, 407–425. [CrossRef]

60. Scott, J.H.; Burgan, R.E. *Standard Fire Behavior Fuel Models: A Comprehensive Set for Use with Rothermel's Surface Fire Spread Model (RMRS-GTR-153)*; USDA Forest Service: Fort Collins, CO, USA, 2005.

61. Lasaponara, R.; Lanorte, A.; Pignatti, S. Characterization and Mapping of Fuel Types for the Mediterranean Ecosystems of Pollino National Park in Southern Italy by Using Hyperspectral MIVIS Data. *Earth Interact.* **2006**, *10*, 1–11. [CrossRef]

62. Ottmar, R.D.; Sandberg, D.V.; Riccardi, C.L.; Prichard, S.J. An overview of the Fuel Characteristic Classification System—Quantifying, classifying, and creating fuelbeds for resource planning. *Can. J. For. Res.* **2007**, *37*, 2383–2393. [CrossRef]

63. Wagenbrenner, N.S.; Forthofer, J.M.; Lamb, B.K.; Shannon, K.S.; Butler, B.W. Downscaling surface wind predictions from numerical weather prediction models in complex terrain with WindNinja. *Atmos. Chem. Phys.* **2016**, *16*, 5229–5241. [CrossRef]

64. Finney, M.A. Fire growth using minimum travel time methods. *Can. J. For. Res.* **2002**, *32*, 1420–1424. [CrossRef]

65. Richards, G.D. An elliptical growth model of forest fire fronts and its numerical solution. *Int. J. Numer. Methods Eng.* **1990**, *30*, 1163–1179. [CrossRef]

66. Rothermel, R.C. *A Mathematical Model for Predicting Fire Spread in Wildland Fuels*; USDA Forest Service, Intermountain Forest and Range Experiment Station: Fort Collins, CO, USA, 1972.

67. Van Wagner, C.E. Conditions for the start and spread of crown fire. *Can. J. For. Res.* **1977**, *7*, 23–34. [CrossRef]

68. Carmel, Y.; Paz, S.; Jahashan, F.; Shoshany, M. Assessing fire risk using Monte Carlo simulations of fire spread. *For. Ecol. Manag.* **2009**, *257*, 370–377. [CrossRef]

69. Knight, I.; Coleman, J. A fire perimeter expansion algorithm-based on Huygens wavelet propagation. *Int. J. Wildland Fire* **1993**, *3*, 73–84. [CrossRef]

70. LaCroix, J.J.; Ryu, S.-R.; Zheng, D.; Chen, J. Simulating fire spread with landscape management scenarios. *For. Sci.* **2006**, *52*, 522–529.

71. Massada, A.B.; Radeloff, V.C.; Stewart, S.I.; Hawbaker, T.J. Wildfire risk in the wildland—Urban interface: A simulation study in northwestern Wisconsin. *For. Ecol. Manag.* **2009**, *258*, 1990–1999. [CrossRef]

72. Sanderlin, J.C.; Van Gelder, R.J. A simulation of fire behavior and suppression effectiveness for operation support in wildland fire management. In Proceedings of the 1st International Conference on Mathematical Modeling, Huajuapan de León, Oaxaca, Mexico, 13–14 November 2014; pp. 619–630.

73. Ager, A.A.; Vaillant, N.M.; Finney, M.A.; Preisler, H.K. Analyzing wildfire exposure and source—Sink relationships on a fire prone forest landscape. *For. Ecol. Manag.* **2012**, *267*, 271–283. [CrossRef]

74. Finney, M.A.; Grenfell, I.C.; McHugh, C.W.; Seli, R.C.; Trethewey, D.; Stratton, R.D.; Brittain, S. A method for ensemble wildland fire simulation. *Environ. Model. Assess.* **2011**, *16*, 153–167. [CrossRef]

75. Arca, B.; Duce, P.; Pellizzaro, G.; Laconi, M.; Salis, M.; Spano, D. Evaluation of FARSITE simulator in Mediterranean shrubland. *For. Ecol. Manag.* **2006**, *234*, S110. [CrossRef]

76. Chiono, L.A.; Fry, D.L.; Collins, B.M.; Chatfield, A.H.; Stephens, S.L. Landscape-scale fuel treatment and wildfire impacts on carbon stocks and fire hazard in California spotted owl habitat. *Ecosphere* **2017**, *8*. [CrossRef]

77. Lydersen, J.M.; Collins, B.M.; Knapp, E.E.; Roller, G.B.; Stephens, S. Relating fuel loads to overstorey structure and composition in a fire-excluded Sierra Nevada mixed conifer forest. *Int. J. Wildland Fire* **2015**, *24*, 484–494. [CrossRef]

78. Maguya, A.S.; Tegel, K.; Junttila, V.; Kauranne, T.; Korhonen, M.; Burns, J.; Leppanen, V.; Sanz, B. Moving Voxel Method for Estimating Canopy Base Height from Airborne Laser Scanner Data. *Remote Sens.* **2015**, *7*, 8950–8972. [CrossRef]

79. Kramer, H.; Collins, B.; Kelly, M.; Stephens, S. Quantifying Ladder Fuels: A New Approach Using LiDAR. *For. Trees Livelihoods* **2014**, *5*, 1432–1453. [CrossRef]

80. Agee, J.K.; Skinner, C.N. Basic principles of forest fuel reduction treatments. *For. Ecol. Manag.* **2005**, *211*, 83–96. [CrossRef]

81. Menning, K.M.; Stephens, S.L. Fire Climbing in the Forest: A Semiqualitative, Semiquantitative Approach to Assessing Ladder Fuel Hazards. *West. J. Appl. For.* **2007**, *22*, 88–93.

82. Dubayah, R.O.; Drake, J.B. Lidar Remote Sensing for Forestry. *J. For.* **2000**, *98*, 44–46.

83. Bye, I.J.; North, P.R.J.; Los, S.O.; Kljun, N.; Rosette, J.A.B.; Hopkinson, C.; Chasmer, L.; Mahoney, C. Estimating forest canopy parameters from satellite waveform LiDAR by inversion of the FLIGHT three-dimensional radiative transfer model. *Remote Sens. Environ.* **2017**, *188*, 177–189. [CrossRef]

84. Peterson, B. Canopy Fuels Inventory and Mapping Using Large-Footprint LiDAR. Ph.D. Thesis, University of Maryland, College Park, MD, USA, 2005.

85. McMahon, S.M.; Bebber, D.P.; Butt, N.; Crockatt, M.; Kirby, K.; Parker, G.G.; Riutta, T.; Slade, E.M. Ground based LiDAR demonstrates the legacy of management history to canopy structure and composition across a fragmented temperate woodland. *For. Ecol. Manag.* **2015**, *335*, 255–260. [CrossRef]

86. De Almeida, D.R.A.; Nelson, B.W.; Schietti, J.; Gorgens, E.B.; Resende, A.F.; Stark, S.C.; Valbuena, R. Contrasting fire damage and fire susceptibility between seasonally flooded forest and upland forest in the Central Amazon using portable profiling LiDAR. *Remote Sens. Environ.* **2016**, *184*, 153–160. [CrossRef]

87. Tempel, D.J.; Gutiérrez, R.J.; Battles, J.J.; Fry, D.L.; Su, Y.; Guo, Q.; Reetz, M.J.; Whitmore, S.A.; Jones, G.M.; Collins, B.M.; et al. Evaluating short- and long-term impacts of fuels treatments and simulated wildfire on an old-forest species. *Ecosphere* **2015**, *6*, art261. [CrossRef]

88. Brosofske, K.D.; Froese, R.E.; Falkowski, M.J.; Banskota, A. A Review of Methods for Mapping and Prediction of Inventory Attributes for Operational Forest Management. *For. Sci.* **2014**, *60*, 733–756. [CrossRef]

89. Woods, M.; Pitt, D.; Penner, M.; Lim, K.; Nesbitt, D.; Etheridge, D.; Treitz, P. Operational implementation of a LiDAR inventory in Boreal Ontario. *For. Chron.* **2011**, *87*, 512–528. [CrossRef]